

## PATH EFFECTS ON PREDICTION EQUATIONS OF PSEUDO-VELOCITY RESPONSE SPECTRA IN NORTHERN JAPAN

Y. P. Dhakal<sup>1</sup>, N. Takai<sup>2</sup> and T. Sasatani<sup>3</sup>

<sup>1</sup> Graduate student, Graduate School of Engineering, Hokkaido University, Sapporo, Japan

<sup>2</sup> Assoc. Professor, Graduate School of Engineering, Hokkaido University, Sapporo, Japan

<sup>3</sup> Professor, Graduate School of Engineering, Hokkaido University, Sapporo, Japan

Email: ypdhakal@eng.hokudai.ac.jp, tki@eng.hokudai.ac.jp, sasatani@eng.hokudai.ac.jp

### ABSTRACT :

We perform regression analysis of pseudo-velocity response spectra of strong ground motions in the period range from 0.1 to 5.0 s by considering two different prediction equations: the first equation consists of a single term of anelastic attenuation and the second equation consists of two-term of anelastic attenuation. Strong-motion records from interplate and intraslab events with  $M_w \geq 5.0 \sim 7.3$  and hypocenter distances less than 300 km are used. Regression analysis results show that the standard errors are significantly reduced by the second prediction equation in the short periods less than about 1 s. The standard errors from the both prediction equations are nearly the same for period longer than 1 s. Finally, the anelastic attenuation coefficients obtained from the second prediction equation are discussed in terms of the different frequency dependency of the quality factor  $Q$  in the fore-arc and back-arc mantle wedges in northern Japan.

**KEYWORDS:** Path effect, Volcanic front, Q-value, Attenuation, Response spectra

### 1. INTRODUCTION

Path effects describe decrease in amplitude of seismic waves with distance. Geometrical spreading and anelastic attenuation are the two factors that contribute to the path effects. In the near field, geometrical spreading plays a major role in decreasing the amplitude of seismic waves whereas the effects of anelastic attenuation become significant at a long distance. Many empirical prediction equations describe the anelastic attenuation by a single term  $bR$ , where  $b$  is a function of period and  $R$  is the source-to-site distance.

There exists heterogeneous attenuation structure beneath northern Japan; the volcanic front has been considered to be the boundary (e.g., Yoshimoto *et al.*, 2006; Figure 1b). It is well known that this structure causes the abnormal seismic intensity distribution in northern Japan (Figure 1a). Recently Morikawa *et al.* (2006) and Kanno *et al.* (2006) proposed correction terms in the prediction equations of PGA, PGV and acceleration response spectra to take the heterogeneous attenuation structure into consideration. However, their prediction equations still assumed the single term of anelastic attenuation. On the other hand, Takai and Okada (2002) developed the prediction equation of seismic intensity by dividing the source-to-site distance into two distances at the volcanic front. They introduced two terms of anelastic attenuation,  $b_1R_1$  and  $b_2R_2$ , where  $R_1$  and  $R_2$  denote the distance from the hypocenter to the volcanic front and distance from the volcanic front to the site (Figure 1b). In the figure and hereafter we denote the fore-arc and back-arc mantle wedges by FAMW and BAMW, respectively.

In this paper, we study path effects on prediction equations of pseudo-velocity response spectra in northern Japan. First we obtain two kinds of prediction equation assuming the single term anelastic attenuation and two-term anelastic attenuation developed by Takai and Okada (2002). Next we compare the results of regression analysis for two kinds of prediction equation. Finally we discuss a meaning of the regression coefficients of two-term anelastic attenuation.

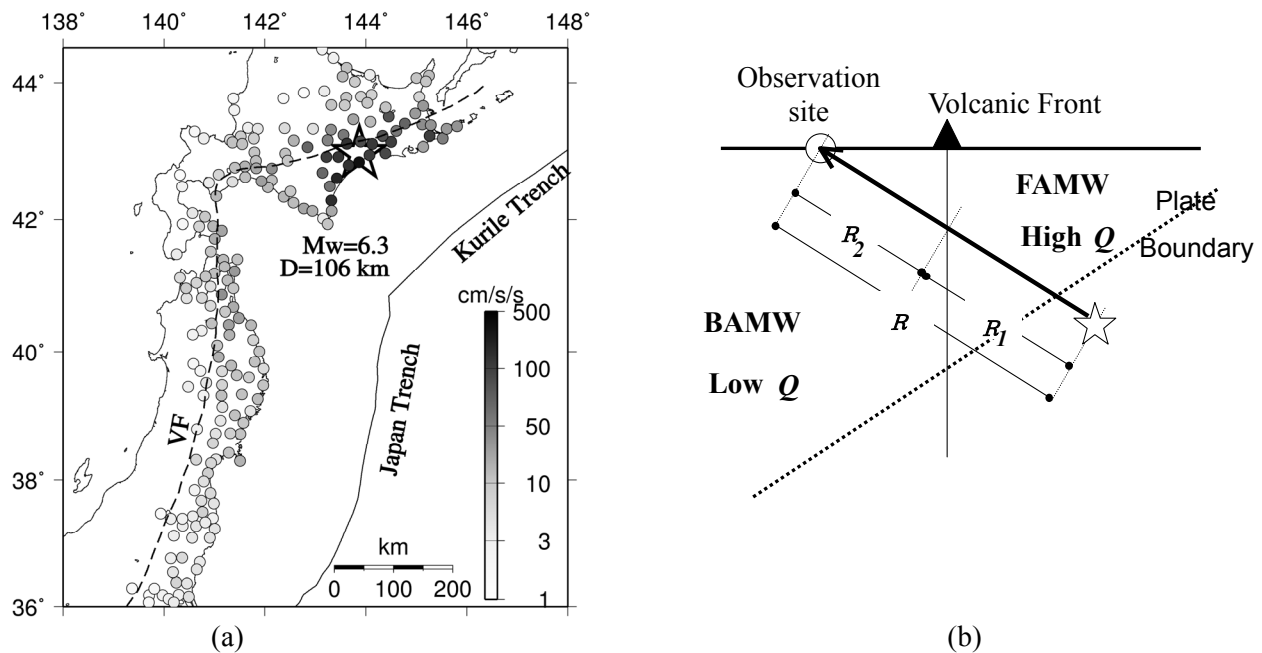


Figure 1 (a) Spatial distribution of peak horizontal accelerations from an intraslab earthquake that occurred in 1999/05/13. JMA epicenter is denoted by a star symbol. VF denotes the volcanic front (dashed line). (b) Schematic vertical section perpendicular to the Japan trench.  $R$ ,  $R_1$  and  $R_2$  are defined in Section 3. FAMW and BAMW denote the fore-arc and back-arc mantle wedges, respectively.  $Q$  denotes a quality factor.

## 2. STRONG GROUND MOTION DATA

Strong ground motion records from K-NET are used. We select earthquakes which satisfy the following criteria: (1) moment magnitude greater than 5 and (2) available records over 50 stations. However, to remove the bias of a large number of records in the fore-arc side compared to the records in the back-arc, only those earthquakes, for which 40% of the records for each event are available from back-arc within a radius of 300 km from the hypocenter, are selected. This condition results in less than 50 records for some events as some stations lie beyond 300 km, the maximum distance considered in this study. We use the interplate and intraslab events occurring in the fore-arc region so that effect of the low  $Q$  zone in BAMW on the back-arc side records can be well accommodated when the seismic waves pass through the volcanic front.

We assume that peak response values are due to the S-wave motion. From this assumption, we select the maximum distance of 300 km in the regression analysis. For smaller magnitude earthquakes we confirmed that the peak responses are due to the S-wave motion. Mw 8 class earthquakes radiate strong surface waves (e.g., Maeda and Sasatani, 2008) and our assumption of peak responses from the S-wave motion may not be valid. Therefore, to make a consistent database, we do not include the magnitude 8 class events in our database. The maximum magnitude for interplate events is Mw 7.3 and the maximum available magnitude for intraslab events is Mw 7 in this study.

The lists of used earthquakes are provided in Tables 1 and 2 for intraslab and interplate events, respectively. The hypocenter information are taken from Japan Meteorological Agency (JMA) and F-net of National Research Institute for Earth Science and Disaster Prevention (NIED). The number of 772 records from 10 events is used for intraslab earthquakes and 1749 records from 20 events are used for interplate earthquakes. The epicenter locations of the earthquakes are shown in Figure 2.

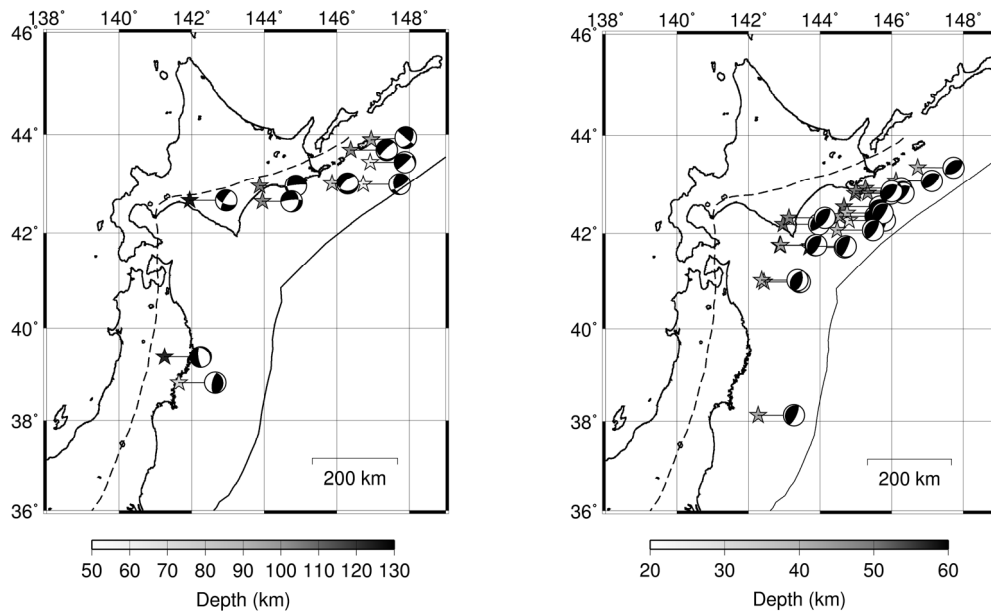


Figure 2 Location maps of (a) intraslab and (b) interplate events used in this study. Stars denote the epicenters. The beach balls connected to the epicenters show the focal mechanisms.

Table 1 List of intraslab earthquakes.

No.	Date and time (JST)	Longitude	Latitude	Mw	D (km)	Stations used	Source
1	1999/05/13 02:59	143.87	42.97	6.1	106	96	JMA
2	2000/01/28 23:21	146.73	43.00	6.8	59	44	JMA
3	2001/04/27 02:49	145.87	43.02	6.0	80	61	JMA
4	2001/12/02 22:02	141.25	39.38	6.3	122	136	JMA
5	2002/12/01 18:57	143.95	42.65	5.4	103	58	JMA
6	2003/05/26 18:24	141.65	38.82	7.0	72	151	JMA
7	2004/11/04 23:03	146.92	43.45	5.8	60	32	JMA
8	2005/09/21 11:25	146.38	43.70	5.9	103	35	JMA
9	2006/11/22 20:15	146.95	43.90	5.6	96	31	JMA
10	2007/04/19 00:07	141.95	42.67	5.5	126	132	JMA

Table 2 List of interplate earthquakes.

No.	Date and time (JST)	Longitude	Latitude	Mw	D (km)	Stations used	Source
1	1997/02/20 16:55	142.87	41.75	6.0	49	119	JMA
2	2001/08/14 05:11	142.43	40.98	6.3	38	160	JMA
3	2001/08/24 18:48	142.37	41.02	5.1	41	65	JMA
4	2002/08/25 03:41	146.12	43.08	6.1	44	44	JMA
5	2003/09/26 06:08	143.69	41.71	7.3	21	170	F-net
6	2003/09/28 07:23	142.97	42.19	5.2	51	57	F-net
7	2003/09/29 11:37	144.55	42.35	6.4	43	80	JMA
8	2003/10/08 18:07	144.67	42.55	6.6	51	64	JMA
9	2003/10/08 22:32	144.81	42.27	5.8	28	49	F-net
10	2003/12/29 10:31	144.75	42.42	6.1	39	63	JMA
11	2004/04/12 03:06	144.98	42.82	6.1	47	59	JMA
12	2004/06/11 03:12	143.13	42.32	5.2	48	98	F-net
13	2004/11/11 19:03	144.48	42.07	6.1	39	77	JMA
14	2004/11/29 03:32	145.27	42.93	7.0	48	87	JMA
15	2004/12/06 23:15	145.33	42.83	6.8	46	89	JMA
16	2005/01/18 23:09	145.00	42.87	6.2	50	78	JMA
17	2005/08/16 11:46	142.27	38.13	7.1	42	146	JMA
18	2006/04/13 13:27	142.894	41.756	5.3	43	75	JMA
19	2007/02/17 09:03	143.723	41.732	5.9	40	130	F-net
20	2007/10/09 02:10	146.727	43.353	5.7	40	39	JMA

### 3. REGRESSION MODEL

Two equations (here after called as Model-1 and Model-2) are used for the regression analysis of the pseudo-velocity response spectra in the period range from 0.1 to 5.0 s useful to the earthquake engineering community. Model-1 has been traditionally used assuming a single term of anelastic attenuation (Eqn. 3.1). Model-2 assumes two terms of anelastic attenuation (Eqn. 3.2).

$$\log_{10}Y(T) = c + aM_w + hD - \log_{10}R - bR \quad (3.1)$$

$$\log_{10}Y(T) = c + aM_w + hD - \log_{10}R - b_1R_1 - b_2R_2 \quad (3.2)$$

where  $a$ ,  $b$ ,  $b_1$ ,  $b_2$ , and  $h$  are regression coefficients,  $c$  is a constant,  $M_w$  is the moment magnitude,  $D$  is the depth of hypocenter;  $R$ ,  $R_1$  and  $R_2$  denote the hypocenter distance, distance from the hypocenter to the volcanic front and distance from the volcanic front to the observation site, respectively (Figure 1b) and  $Y(T)$  is the 5% damped pseudo-velocity response in cm/s calculated as the maximum of the vector sum of two horizontal responses for a natural period  $T$  in second.

### 4. REGRESSION ANALYSIS

Two-step regression analysis method as described by Joyner and Boore (1981) is applied. In the first step, coefficient  $b$  in case of Model-1 and coefficients  $b_1$  and  $b_2$  in case of Model-2 are determined by replacing the constant, magnitude and depth terms with dummy variables as shown in Eqns. 4.1 and 4.2.

$$\log_{10}Y(T) + \log_{10}R = -bR + \sum d_i l_i \quad (4.1)$$

$$\log_{10}Y(T) + \log_{10}R = -b_1R_1 - b_2R_2 + \sum d_i l_i \quad (4.2)$$

where  $l_i$  is a dummy variable equal to 1 for the  $i^{\text{th}}$  earthquake and 0 for others;  $d_i$  is a coefficient for the  $i^{\text{th}}$  earthquake. In the second step, coefficients  $b$ ,  $b_1$  and  $b_2$  are substituted in the base models and the unknown coefficients  $a$  and  $h$  and the constant  $c$  are determined as shown in Eqns. 4.3 and 4.4.

$$\log_{10}Y(T) + \log_{10}R + bR = c + aM_w + hD \quad (4.3)$$

$$\log_{10}Y(T) + \log_{10}R + b_1R_1 + b_2R_2 = c + aM_w + hD \quad (4.4)$$

We make regression analysis separately for the intraslab and interplate events because the source characteristics of the two types of events differ significantly (e.g., Satoh, 2004; Morikawa and Sasatani, 2004).

### 5. RESULTS

The results of regression analysis for Model-2 are presented in Table 3, where  $T$  denotes the natural period and  $\sigma_{\log}$  denotes the standard error of regression. Figure 3a shows standard errors of regression analysis for two models. We can see that standard errors are significantly reduced for periods shorter than about 1.0 s by using Model-2. For periods longer than about 1 s, both models have nearly the similar level of errors. The fore-arc anelastic attenuation coefficient  $b_1$  and the back-arc anelastic attenuation coefficient  $b_2$  have different values for periods less than about 2.0 s for both types of events; but they are nearly equal in the range of 2.0 to 5.0 s (Figure 3b and 3c). The values of  $b_1$  are larger than values of  $b_2$ . The large difference between the two coefficients in the short periods indicates that the rate of attenuation in the FAMW is different from the rate of attenuation in the BAMW.

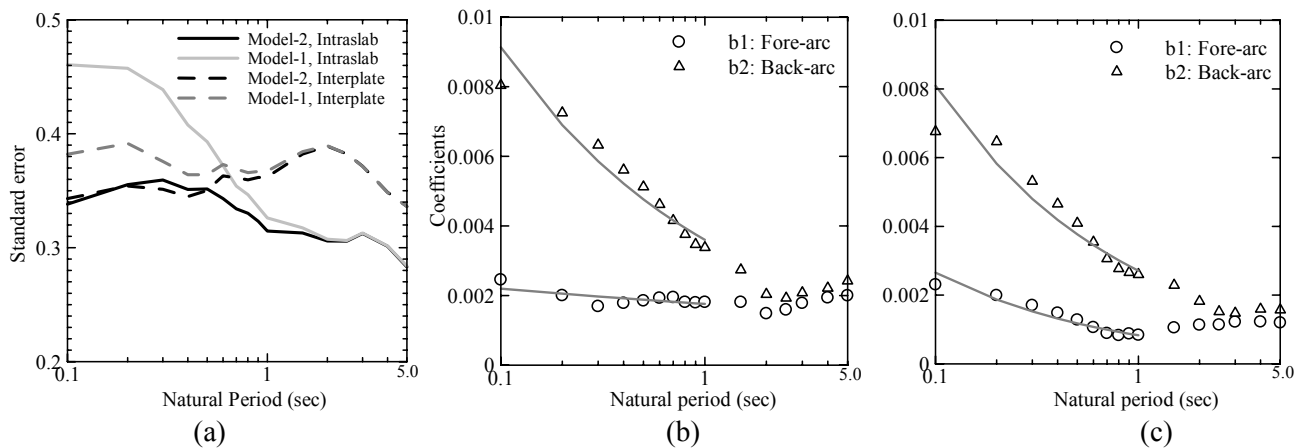


Figure 3 Regression results: (a) standard errors, and  $b_1$  and  $b_2$  for (b) intraslab and (c) interplate events.

The plots of residuals with respect to the hypocenter distances for period of 0.1 and 1.0 s are shown in Figure 4. In the figure, the grey scale bar shows the ratio  $R_1/(R_1+R_2)$  of the fore-arc distance to the hypocenter distance. The ratio equal to 1 implies the fore-arc sites. Figure 4a shows that the distribution of the residuals for period of 0.1 s obtained by using Model-1 is virtually dipolar: positive residuals for the fore-arc sites and negative residuals for the back-arc sites. This systematic alignment of the residuals is removed by using Model-2 and the residuals from the fore-arc and back-arc sites distribute evenly with respect to the hypocenter distance (Figure 4b). As indicated by the similar values of  $b_1$  and  $b_2$  for longer periods (Figures 3b and 3c), both models result in the similar distribution of residuals with respect to the hypocenter distance for the back-arc and the fore-arc sites, as for example, Figures 4c and 4d for period of 1 s.

We make a comparison between the observed and predicted values for period of 0.1 s from Model-2 and the attenuation relation of Kanno *et al.* (2006); in the latter prediction we apply the anomalous correction term for their deep events. Figure 5a shows that Model-2 can predict similar values to the attenuation relation of Kanno *et al.* (2006) (Figure 5b) for intraslab events. However, we can see smaller scattering of the data points by using the Model-2, which considers two terms of anelastic attenuation in the prediction equation. This indicates that the abnormal distribution of strong ground motions observed in northern Japan can be more precisely described by the Model-2 than the correction terms used by Kanno *et al.* (2006).

## 6. DISCUSSION

Trifunac (1976) had described that the  $b$ -values might be considered to be equivalent to  $\pi f \log_{10} e / Q(f) V_s$  i.e.

$$b(f) \sim \pi f \log_{10} e / Q(f) V_s \quad (6.1)$$

where  $f$  is frequency and  $V_s$  is S-wave velocity. Based on the values of  $b_1$  and  $b_2$  obtained by regression analysis, we converted them to the apparent  $Q$ -values by using Eqn. 6.1. The frequency dependency of  $Q$ -value can be expressed in an exponential form as  $Q=Q_0 f^n$  (e.g., Rautin and Khaltrin, 1978), where  $Q_0$  and  $n$  are constants. We fit the similar functional form to the converted  $Q$ -values in the periods of 0.1 to 1 s and the fitted equations for intraslab earthquakes are shown in Eqn. 6.2 and 6.3 for the FAMW and BAMW.  $V_s$  is assumed to be 4 km/s in Eqn. 6.1 to calculate the  $Q$ -values.

$$Q_s (\text{FAMW}) = 194 f^{0.9} \quad (6.2)$$

$$Q_s (\text{BAMW}) = 95 f^{0.59} \quad (6.3)$$

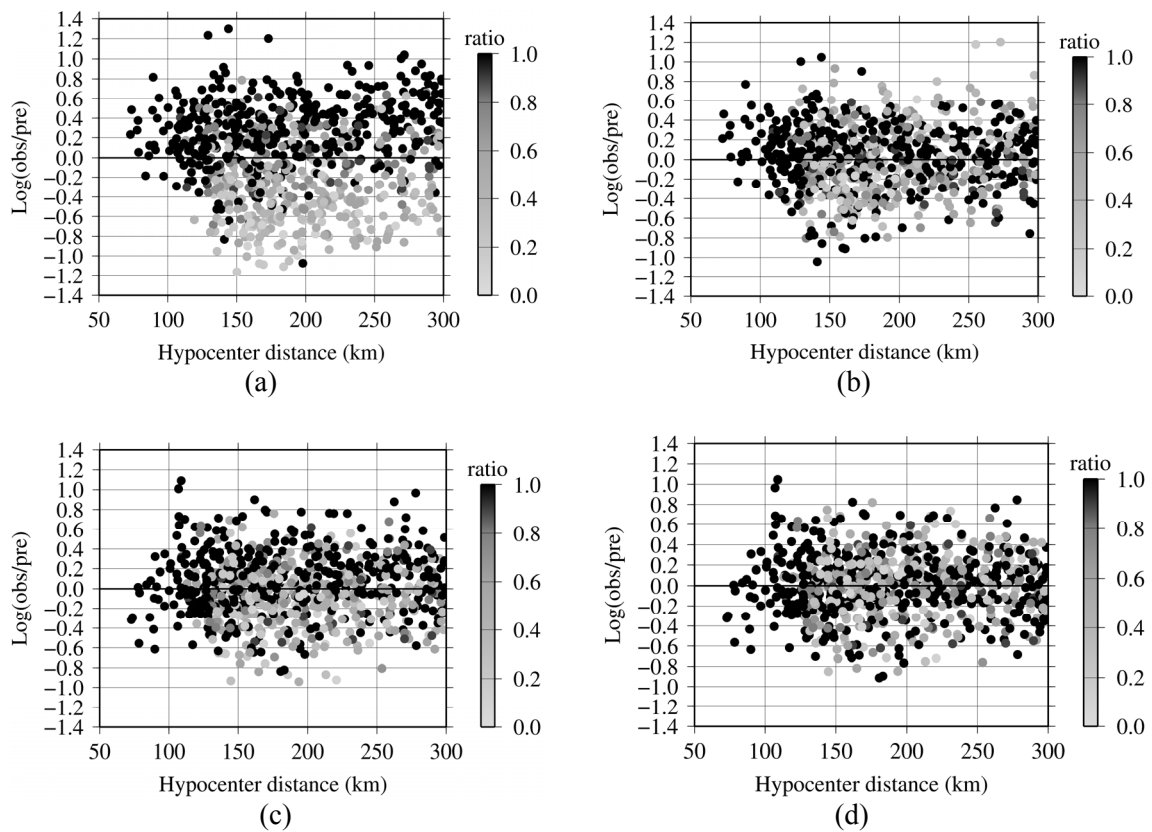


Figure 4 Residuals versus hypocenter distances for period of 0.1 s by using (a) Model-1 and (b) Model-2 and for period of 1.0 s by using (c) Model-1 and (d) Model-2 for intraslab events.

Table 3 Regression coefficients and standard errors by using Model-2.

$T$ (s)	Intraslab earthquakes						Interplate earthquakes					
	$c$	$a$	$h$	$b_1$	$b_2$	$\sigma_{log}$	$c$	$a$	$h$	$b_1$	$b_2$	$\sigma_{log}$
0.1	0.4257	0.4130	-0.0012	0.00245	0.00804	0.34	-1.2558	0.5583	0.0029	0.00230	0.00676	0.34
0.2	0.5884	0.4316	-0.0014	0.00200	0.00725	0.36	-0.6494	0.5346	0.0012	0.00199	0.00647	0.35
0.3	0.1343	0.5047	-0.0011	0.00169	0.00633	0.36	-0.8796	0.5764	0.0019	0.00170	0.00531	0.35
0.4	-0.3562	0.5795	-0.0006	0.00178	0.00561	0.35	-1.0249	0.5999	0.0021	0.00148	0.00465	0.34
0.5	-0.3952	0.5939	-0.0012	0.00185	0.00512	0.35	-1.0792	0.6129	0.0011	0.00128	0.00409	0.35
0.6	-0.6811	0.6270	-0.0007	0.00193	0.00462	0.34	-1.2059	0.6300	0.0007	0.00106	0.00355	0.36
0.7	-1.0857	0.6678	0.0007	0.00195	0.00416	0.33	-1.4175	0.6526	0.0015	0.00089	0.00306	0.36
0.8	-1.3407	0.6917	0.0013	0.00181	0.00376	0.33	-1.6068	0.6749	0.0022	0.00083	0.00277	0.36
0.9	-1.5860	0.7156	0.0020	0.00180	0.00347	0.32	-1.7692	0.6976	0.0027	0.00087	0.00266	0.36
1.0	-1.9269	0.7573	0.0028	0.00181	0.00338	0.31	-1.9573	0.7226	0.0030	0.00084	0.00260	0.36
1.5	-2.3764	0.8184	0.0028	0.00181	0.00274	0.31	-2.4955	0.8005	0.0032	0.00105	0.00229	0.38
2.0	-3.1891	0.9192	0.0032	0.00148	0.00203	0.31	-2.7698	0.8409	0.0021	0.00113	0.00182	0.39
2.5	-3.6913	0.9945	0.0030	0.00159	0.00193	0.31	-2.9862	0.8703	0.0013	0.00114	0.00152	0.38
3.0	-3.9050	1.0277	0.0027	0.00178	0.00208	0.31	-3.1496	0.8914	0.0011	0.00122	0.00147	0.37
4.0	-4.0473	1.0526	0.0016	0.00194	0.00221	0.30	-3.4820	0.9224	0.0018	0.00123	0.00159	0.35
5.0	-4.1328	1.0611	0.0011	0.00200	0.00242	0.28	-3.6811	0.9406	0.0015	0.00120	0.00157	0.34

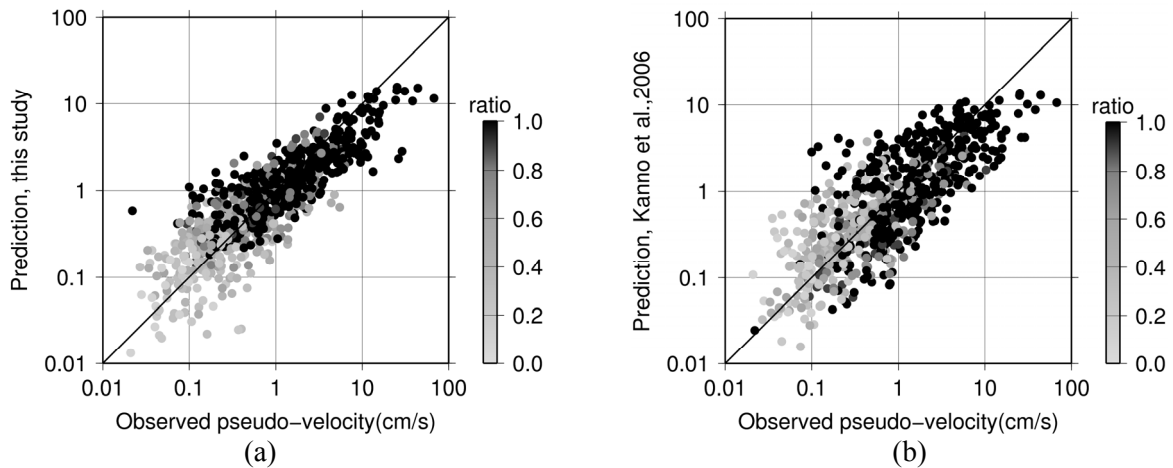


Figure 5 Comparison between predicted and observed values for period of 0.1 s for intraslab events; (a) this study and (b) attenuation relation of Kanno *et al.* (2006).

The lines in Figure 5 show the trend of the  $b$ -values obtained by using Eqn. 6.1 and the  $Q$ -values from the above two equations (Eqns. 6.2 and 6.3). Apparently high  $Q$ -values and strong frequency dependency is found for the FAMW as compared to the BAMW. Similarly Eqns. 6.4 and 6.5 show the frequency dependency of the  $Q$ -value derived from the interplate events for the FAMW and the BAMW in the periods of 0.1 to 1 s.

$$Q_s(\text{FAMW}) = 411f^{0.49} \quad (6.4)$$

$$Q_s(\text{BAMW}) = 126f^{0.52} \quad (6.5)$$

Both earthquake types produce nearly the similar frequency dependency of the  $Q$ -value for the BAMW. However they show different dependencies for the FAMW. The difference may be interpreted by the fact that the  $Q$ -values derived from the intraslab events represent the path averaged values for the mantle wedge including a larger and deeper portion of the subducting slab whereas the  $Q$ -values from the interplate events mostly represent the path averaged values for the mantle wedge and upper portion of the slab. These results are similar to the findings from other studies like Maeda and Sasatani (2006), who obtained high  $Q$ -values and large frequency dependency in the pacific slab near the southern Kurile trench. The intermediate  $Q$ -values for the mantle wedge in the fore-arc for interplate earthquakes agree to the intermediate  $Q$ s values as indicated by Umino and Hasegawa (1984) for the mantle wedge between the Pacific coast and the volcanic front.

## 7. CONCLUSION

Path effects can be more accurately represented by two-term of anelastic attenuation in prediction equations for periods of 0.1 to 1.0 s in northern Japan, where a distinct attenuation boundary separating low  $Q$  and high  $Q$  zones exists. This will eliminate the additional correction term in the prediction models. The different attenuation coefficients for the fore-arc and the back-arc may be interpreted in terms of the different frequency dependency of the  $Q$ -values in the FAMW and the BAMW of northern Japan.  $Q$ -values are strongly frequency dependant in the FAMW as inferred from the anelastic attenuation coefficients in the periods from 0.1 to about 1 s. The frequency dependency of  $Q$ -values is smaller in the BAMW. High frequency strong ground motions are recorded in wide areas of the fore-arc due to the smaller attenuation effect of the large frequency dependency of the  $Q$ -value in the FAMW; but the high frequency components of seismic waves are strongly attenuated in the back-arc when they travel through the volcanic front. However, there has been no remarkable effect of the volcanic front on the long-period ground motions in the back-arc region and the two models (Model-1 and Model-2) describe similar path effects.

## ACKNOWLEDGEMENT

We are thankful to National Institute for Earth Science and Disaster Prevention, which provided strong motion data. We are thankful to Japan Meteorological Agency, which provided the hypocenter information. Center for Engineering Education Development, Hokkaido University, is acknowledged for the partial support to attend this conference. We are also thankful to Wessel and Smith for freely availing Generic Mapping Tool, which is used to make some of the figures in this paper.

## REFERENCES

- F-net. <http://www.hinet.bosai.go.jp/fnet>, last accessed-06/18/2008.
- JMA-CMT Catalog. <http://www.seisvol.kishou.go.jp>, last accessed-06/18/2008.
- Joyner, W. B. and Boore, D. M. (1981). Peak horizontal acceleration and velocity from strong motion records including records from the 1979 Imperial Valley, California, earthquake. *Bulletin of the Seismological Society of America* **71**, 2011-2038.
- Kanno, T., Narita, A., Morikawa, N., Fujiwara, H. and Fukushima, Y. (2006). A New Attenuation Relation for Strong Ground Motion in Japan Based on Recorded Data. *Bulletin of the Seismological Society of America* **96**, 879-897.
- K-NET. <http://www.k-net.bosai.go.jp>, last accessed-06/15/2008.
- Maeda, T. and Sasatani, T. (2006). Two-layer Qs structure of the slab near the southern Kurile trench. *Earth Planets Space* **58**, 543-553.
- Maeda, T. and Sasatani, T. (2008). Long-period ground motions from the 2003 Tokachi-oki earthquake. *Journal of Seismology* **12**, 243-255.
- Morikawa, N. and Sasatani, T. (2004). Source models of two large intraslab earthquakes from broadband strong ground motions. *Bulletin of the Seismological Society of America* **94**, 803-817.
- Morikawa N., Kanno, T., Narita A., Fujiwara, H. and Fukushima, Y. (2006). New additional correction terms for attenuation relations of peak amplitudes and response spectra corresponding to the anomalous seismic intensity in northeastern Japan. *Journal of Japan Association of Earthquake Engineering* **6**, 23-40 (in Japanese with English abstract).
- Rautian, T. G. and Khalturin, V. I. (1978). The use of the coda for determination of the earthquake source spectrum. *Bulletin of the Seismological Society of America* **68**, 923-948.
- Satoh, T. (2004). Short-period spectral level of intraplate and interplate earthquakes occurring off Miyagi prefecture. *Journal of Japan Association of Earthquake Engineering* **4**, 1-4 (in Japanese with English abstract).
- Takai, N. and Okada, S. (2002). Improvement of attenuation formula of earthquake ground motion in consideration of the volcanic front. **11<sup>th</sup> Earthquake Engineering Symposium**, Japan, proceedings: 605-608 (in Japanese with English abstract).
- Trifunac, M. D. (1976). Preliminary empirical model for scaling fourier amplitude spectra of strong ground acceleration in terms of earthquake magnitude, source-to-station distance, and recording site conditions. *Bulletin of the Seismological Society of America* **66**, 1343-1373.
- Umino, N. and Hasegawa, A. (1984). Three-dimensional Qs structure in the northeastern Japan arc, *Zisin* **37**, 213-228 (in Japanese with English abstract).
- Wessel, P. and Smith, W. H. F. (1998). New improved version of the generic mapping tools released. *Eos Transactions American Geophysical Union* **79**, 579.
- Yoshimoto, K., Wegler, U. and Korn, M. (2006). A volcanic front as a boundary of seismic attenuation structures in northeastern Honshu, Japan. *Bulletin of the Seismological Society of America* **96**, 637-646.